



HAL
open science

X-Ray diffraction structure of Cu(II) and Zn(II) complexes of 8-aminoquinoline derivatives (TDMQ), related to the activity of these chelators as potential drugs against Alzheimer's disease

Youzhi Li, Michel Nguyen, Laure Vendier, Anne Robert, Yan Liu, Bernard Meunier

► **To cite this version:**

Youzhi Li, Michel Nguyen, Laure Vendier, Anne Robert, Yan Liu, et al.. X-Ray diffraction structure of Cu(II) and Zn(II) complexes of 8-aminoquinoline derivatives (TDMQ), related to the activity of these chelators as potential drugs against Alzheimer's disease. *Journal of Molecular Structure*, 2022, 1251, pp.132078. 10.1016/j.molstruc.2021.132078 . hal-03509314

HAL Id: hal-03509314

<https://hal.science/hal-03509314v1>

Submitted on 31 May 2022

HAL is a multi-disciplinary open access archive for the deposit and dissemination of scientific research documents, whether they are published or not. The documents may come from teaching and research institutions in France or abroad, or from public or private research centers.

L'archive ouverte pluridisciplinaire **HAL**, est destinée au dépôt et à la diffusion de documents scientifiques de niveau recherche, publiés ou non, émanant des établissements d'enseignement et de recherche français ou étrangers, des laboratoires publics ou privés.

X-Ray diffraction structure of Cu(II) and Zn(II) complexes of 8-aminoquinoline derivatives (TDMQ), related to the activity of these chelators as potential drugs against Alzheimer's disease

Youzhi Li,^{a,b,c} Michel Nguyen,^{b,c} Laure Vendier,^b Anne Robert,^{b,c,*} Yan Liu,^{a,*} Bernard Meunier,^{a,b,c}

^a Guangdong University of Technology, School of Chemical Engineering and Light Industry, no. 100 Waihuan Xi road, Education Mega Center, Guangzhou, P. R. China.

^b Laboratoire de Chimie de Coordination du CNRS, 205 route de Narbonne, BP 44099, 31077 Toulouse cedex 4, France.

^c New antimalarial molecules and pharmacological approaches, Inserm ERL 1289, 205 route de Narbonne, BP 44099, 31077 Toulouse cedex 4, France.

E-mail: anne.robert@lcc-toulouse.fr, yanliu@gdut.edu.cn

Highlights

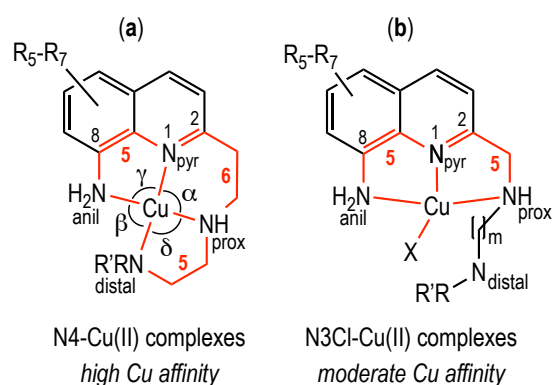
- TDMQ, regulators of copper homeostasis as drug-candidates against Alzheimer's disease
- The definition of the coordination sphere of TDMQ chelators is crucial for regulation of Cu homeostasis
- A N4-square planar X-ray structure of Cu-TDMQ complexes is required
- Specificity of TDMQ ligands for Cu(II) with respect to low affinity for Zn(II)

Abstract

TDMQ chelators have been designed as drug-candidates for the regulation of copper homeostasis and for the reduction of the oxidative stress in the brain of Alzheimer's patients. To achieve suitable biological properties and high Cu(II) selectivity in a zinc-rich medium, TDMQ ligands must meet critical coordination chemistry requirements related to the structures of the Cu^{II}-TDMQ complexes. The correlation between X-ray diffraction structures of Cu- and

Zn-TDMQ complexes and their physicochemical properties should therefore help to draw pertinent correlations between structure and properties of the drug-candidates, and to select the most promising ones for biological studies. Here we report the X-ray structures of single crystals of Cu-TDMQ36, and of the zinc complexes of TDMQ35, TDMQ36 and TDMQ22. Comparison with the already reported structures of other copper and zinc complexes of TDMQ then allows to specify the structure requirement for potentially more efficient drugs.

Graphical abstract



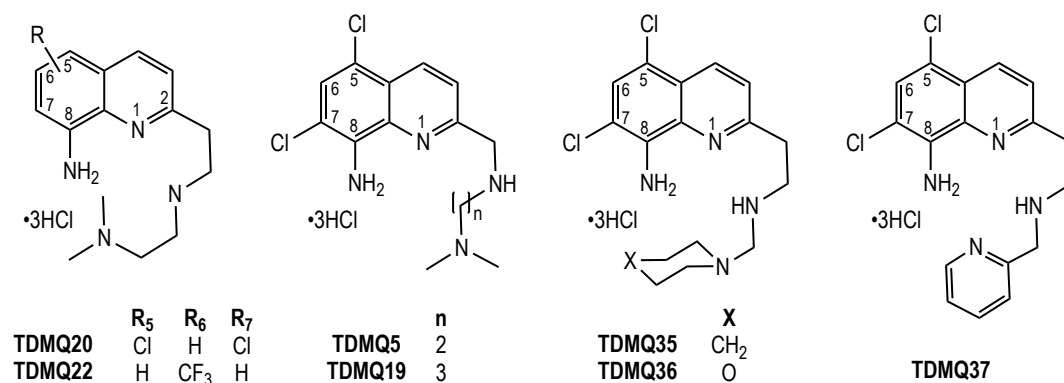
Keywords

Alzheimer's disease; Copper chelator; 8-Aminoquinoline; X-Ray crystallography; Zinc.

Introduction

The search for efficient drugs able to stop the cognitive decline of Alzheimer's disease (AD) at the early stages is one of the most challenging topics in medicinal chemistry [1]. The detrimental redox effect of the disruption of copper homeostasis in AD brain has been considered as a valuable target. Then, design of specific chelators able to inhibit the catalytic reduction of dioxygen produced by copper-loaded amyloids (Cu-A β) is a promising way [2, 3]. Such ligands must be specific for Cu(II) with respect to Zn(II) in order to avoid the neurotoxicity due to chelation of zinc, that was a feature of first generation of metal chelators like clioquinol or PBT2, based on a non-specific 8-hydroxyquinoline motif [4]. We have identified a series of tetradentate ligands based on a 8-aminoquinoline scaffold bearing an aliphatic polyamine chelating side chain, named TDMQ (for the structures of some of these TDMQ ligands, see Scheme 1) [5]. One of these copper ligands, TDMQ20, is highly efficient to rescue the declarative memory impairment in a robust non-transgenic murine model of AD, and to reduce the oxidative stress in mouse cortex [6]. Many of these TDMQ ligands are also specific for Cu(II) with respect to Zn(II), their affinity for Cu(II) being 10 log higher than that for Zn(II) [5a].

In order to achieve high Cu(II) selectivity and suitable biological properties, the design of TDMQ chelators must meet some critical coordination chemistry requirements related to the structures of the Cu^{II}-TDMQ complexes. The correlation between X-ray diffraction structures of Cu- and Zn-TDMQ complexes and their physicochemical properties should therefore help to draw pertinent correlations between structure and properties of the drugs, and to select the most promising ones for biological and pharmacological studies.



Scheme 1. Structures of TDMQ ligands. The X-ray structures of Cu-TDMQ36, Zn-TDMQ35, Zn-TDMQ36, and Zn-TDMQ22 are described in this report. Other structures, previously reported in References 5a, 5c and 7, are used for comparison (see Table 1).

We report here the X-ray structure of single crystals of Cu-TDMQ36, and that ones of the zinc complexes of TDMQ35, TDMQ36 and TDMQ22. Comparison with the already reported structures of other copper and zinc complexes of TDMQ [5a, 2b, 7] then will allow to specify the structure requirement for potentially efficient drugs.

Results and discussion

X-Ray structure of Cu-TDMQ36

Single crystals of Cu^{II}-TDMQ36 (Figure 1) were obtained by slow evaporation in air at room temperature of a DMF/ethanol (1/3, v/v) filtered solution containing an equimolecular mixture of CuCl₂ and TDMQ36 (32 mM) in the presence of triethylamine (3 mol equiv). The space group was *P*2₁/*c*. In each Cu-TDMQ36 motif, Cu(II) was chelated by the four nitrogen atoms of the ligand: N_{pyridine}, N_{aniline}, and the N_{proximal} and N_{distal} of the side chain. The aniline nitrogen was not deprotonated, and a chloride anion and a water molecule were bound as axial ligands ($d_{\text{Cu-Cl}} = 2.810 \text{ \AA}$, $d_{\text{Cu-O}} = 2.730 \text{ \AA}$, $\text{H}_2\text{O-Cu-Cl}$ angle = 164.04°). Electroneutrality of the unit cell was achieved by the presence of another chloride ion. The N₄ square plane around copper was nearly perfect. The length of the bonds between Cu and nitrogens were quite similar, measured at 2.031, 2.024, 2.212, and 2.080 \AA for N_{pyridine}, N_{aniline}, N_{proximal} and N_{distal}, respectively. The N-Cu-N angles in the base plane were N_{pyridine}-Cu-N_{aniline} (γ) = 89.43° , N_{proximal}-Cu-N_{distal} (δ) = 85.94° , N_{aniline}-Cu-N_{distal} (β) = 96.25° , and N_{pyridine}-Cu-N_{proximal} (α) = 93.99° . The dihedral angles between N_{pyridine}-Cu-N_{aniline} and N_{proximal}-Cu-N_{distal}, N_{pyridine}-Cu-N_{aniline} and N_{pyridine}-Cu-N_{proximal}, and N_{pyridine}-Cu-N_{proximal} and N_{proximal}-Cu-N_{distal} were 6.43° , 4.45° , and 4.96° , respectively. The copper was located at 0.084 \AA above the mean plane of the four nitrogen atoms, slightly driven by the axial chloride. Noteworthy, the oxygen atom of the morpholine residue did not take part in metal chelation.

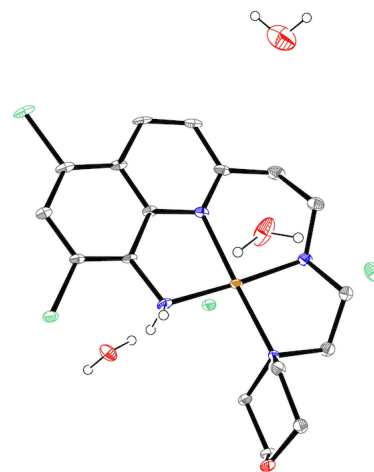
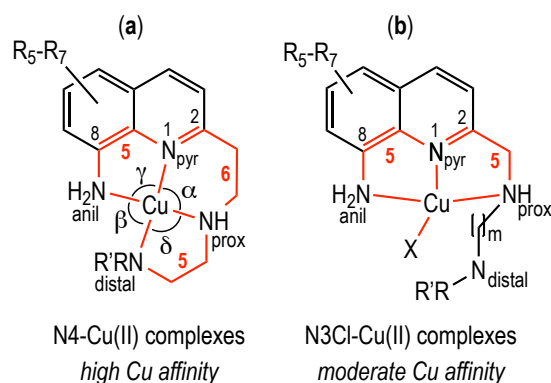


Figure 1. ORTEP drawing with ellipsoids at 30% probability of the X-ray diffraction structure of the Cu^{II}-TDMQ36 complex.

Moreover, the three-dimensional structure of Cu^{II}-TDMQ36 exhibits numerous standard hydrogen interactions of the N-H \cdots O and O-H \cdots O type, and also halogen-hydrogen bonds O-

H...Cl depicted in Table S1 and Figure S1. This gives rise to an infinite sequence in the three directions and contributes to the supramolecular arrangement.

This structure is consistent with the previously reported X-ray diffraction structures of the Cu(II) complexes of TDMQ20 [2b], TDMQ22 [5a] and TDMQ37 [7] (Table 1). Like TDMQ22, these ligands exhibit a side chain suitable perfect square planar coordination sphere of Cu(II) by the four nitrogen atoms of the ligand, that designed cycles $N_{\text{aniline}}\text{-Cu-}N_{\text{pyridine}}$, $N_{\text{pyridine}}\text{-Cu-}N_{\text{proximal}}$, and $N_{\text{proximal}}\text{-Cu-}N_{\text{distal}}$ exhibiting 5, 6, and 5 bonds, respectively



Scheme 2. Two different types of coordination of Cu(II) by TDMQ ligands, depending on the structure of the side chain.

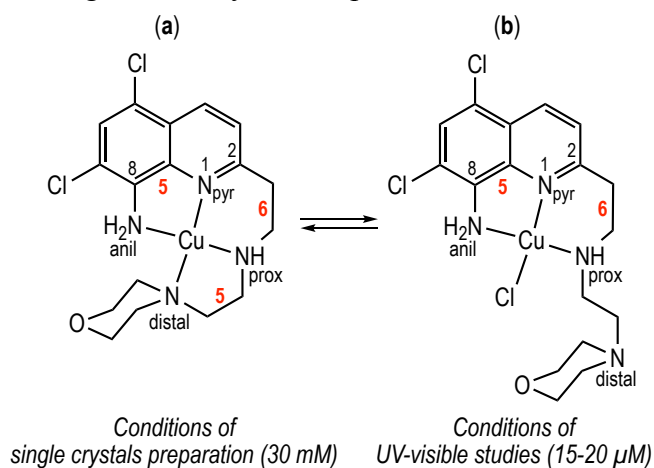
(Scheme 2a). This preferred coordination of Cu(II) consequently resulted in the high affinity of such ligands for Cu(II) ($\log K_{\text{app}} = 16.5$, and 17.1 for TDMQ20 [2b], and TDMQ37 [7], respectively). Conversely, TDMQ ligands having a shorter tether between N_{pyridine} and N_{proximal} (TDMQ5 and TDMQ19) that resulted in a 5-membered ring $N_{\text{pyridine}}\text{-Cu-}N_{\text{proximal}}$ (Scheme 2b, [5a]) prevented efficient coordination of N_{distal} whatever the $N_{\text{proximal}}\text{-}N_{\text{distal}}$ length was ($m = 1$ or 3). These latter complexes have a strained N3Cl coordination sphere around Cu(II) and the square plane around Cu(II) is consequently distorted, resulting in a lower affinity for Cu(II) ($\log K_{\text{app}} = 9.8$, and 10.2 for TDMQ5 and TDMQ19, respectively [5a]. The affinity of TDMQ36 has an intermediate value between these two series ($\log K_{\text{app}} = 13.1$ [7]).

TDMQn n =	$\log K_{\text{app}}$ [M-L]		Inhibition of ROS production ^a	X-ray diffraction structures of TDMQ metal complexes	
	Cu	Zn		Cu	Zn
5	9.8 ^b	4.2 ^b	19 % ^b	N3Cl(OH ₂) ^b	N2Cl2 ^b
19	10.2 ^b	< 3 ^b	64 % ^b	N3Cl(Cl) ^b	N2Cl2 ^b
20	16.5 ^b	4.2 ^b	100 % ^b	N4(OH ₂) or (Cl) ^c	N2Cl2 ^b
22	15.1 ^b	4.1 ^b	100 % ^b	N4(Cl)(Cl) ^b	N4(Cl)(Cl-Zn-Cl ₃) ^e
35	13.7 ^d	< 4.7 ^d	80 % ^d	nd	N2Cl2 ^e
36	13.1 ^d	< 5.0 ^d	60 % ^d	N4(OH ₂)(Cl) ^e	N2Cl2 ^e
37	17.1 ^d	5.1 ^d	100 % ^d	N4 ^d	N2Cl2 ^d

^a Measured as inhibition of the aerobic ascorbate oxidation induced by Cu-A β complex. ^b Reference 5a. ^c Reference 2b. ^d Reference 7. ^e This work.

Table 1. Summary of affinity constants of the Cu(II) and Zn(II) complexes of selected TDMQ chelators, correlated with their ability to inhibit the oxidative stress induced by Cu-A β , and with the metal environment in the X-ray diffraction structures of single crystals of these complexes.

The design of TDMQ ligands aimed to inhibit the oxidative stress induced by Cu-amyloid complexes. This property is indirectly evaluated as the ability of these ligands to inhibit ascorbate oxidation in the presence of Cu- $A\beta_{1-16}$ [8]. Due to the high stability of the Cu(II) complexes of the N4-tetradentate TDMQ20, TDMQ22 and TDMQ37, these ligands completely inhibited the ROS production induced by Cu- $A\beta_{1-16}$ [5a, 7]. In similar conditions, the N3Cl ligands TDMQ5 and TDMQ19 were unable to fully result in inhibit ROS production, and ascorbate oxidation was 81 % and 36 %, respectively, after 10 min. On this point of view, TDMQ36 did not efficiently inhibit ROS production, with an ascorbate oxidation at 40 % [7]. UV-visible measurement of affinity constants or ascorbate oxidation were carried out in drastically different conditions than single crystals preparation, particularly with regard to ligand concentration, 30 mM for single crystals preparation and 15-20 μ M for UV-visible studies. Then, we propose that the steric hindrance generated by the morpholine residue resulted in an equilibrium between N3 and N4 chelation of Cu(II) in solution (Scheme 3), this equilibrium being dependent on the ligand concentration and/or the copper/ligand molar ratio. This feature might be responsible for a lower affinity of TDMQ36 for Cu(II) than that of TDMQ20 or TDMQ37, and for a poorly efficient inhibition of ROS production.



Scheme 3. Possible equilibrium in solution between N4- and N3Cl coordination of copper in the Cu^{II}-TDMQ36 complex.

X-Ray structure of Zn-TDMQ35

Slow vapor diffusion of dichloromethane into solution of TDMQ35 and ZnCl₂ (TDMQ35/Zn mole ratio = 2/1) in ethanol at 4 °C afforded single crystals of Zn(II)-TDMQ35. The space group was *P*2₁/*n*. In each ZnTDMQ35 motif, the metal ion

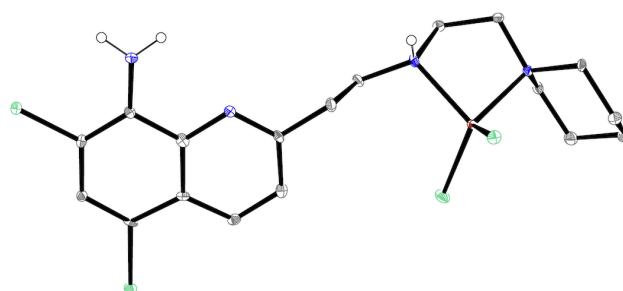


Figure 2. ORTEP drawing with ellipsoids at 30% probability of the Zn^{II}-TDMQ35 complex.

was chelated by the two nitrogen atoms of the ligand side chain and two chloride ligands in a tetrahedral environment (Figure 2) that generally represents the optimal environment of Zn(II) [9]. The aminoquinoline nitrogen atoms did not take part in complexation. The tetrahedron

structure is distorted by the 5-membered $N_{\text{proximal}}\text{-Zn-}N_{\text{distal}}$ ring, with the $N_{\text{proximal}}\text{-Zn-}N_{\text{distal}}$ and Cl-Zn-Cl angles measured at 86.29° and 116.72° , respectively. The length of the bonds between Zn and nitrogen atoms were measured at 2.104 and 2.122 Å for N_{proximal} and N_{distal} , respectively. The length of the Zn–Cl bonds were 2.236 and 2.207 Å for the two chloride ligands. The dihedral angle between $N_{\text{proximal}}\text{-Zn-}N_{\text{distal}}$ and Cl-Zn-Cl planes was 87.21° .

X-Ray structure of Zn-TDMQ36

Slow vapor diffusion of dichloromethane into solution of TDMQ36 and ZnCl_2 (TDMQ36/Zn mole ratio = 1/1) in ethanol at 4°C afforded single crystals of $\text{Zn}^{\text{II}}\text{-TDMQ36}$. The space group was $P2_1/c$. The two Zn-TDMQ36 motifs contained in each unit cell were very close, and similar to that of Zn-TDMQ35, with the metal ion in a distorted tetrahedral N_2Cl_2 environment (Figure 3). The $N_{\text{proximal}}\text{-Zn-}N_{\text{distal}}$ and Cl-Zn-Cl angles measured 87.60° and 118.16° (motif A) or 87.82° and 103.34° (motif B), respectively. The distances between Zn and N_{proximal} and N_{distal} were measured at 2.093 and 2.088 Å, respectively, in motif A), and 2.059 and 2.104 Å, respectively, in motif B. The length of the Zn–Cl bonds were 2.205 and 2.230 Å for the two chloride ligands (motif A), or 2.235 and 2.208 Å, respectively (motif B). The dihedral angles between $N_{\text{proximal}}\text{-Zn-}N_{\text{distal}}$ and Cl-Zn-Cl planes were 84.88° and 83.77° , close to the theoretical value of 90° , in motifs A and B, respectively. In addition, the three-dimensional structure of Zn-TDMQ36 exhibits intra- and inter-molecular hydrogen bonds, of the $\text{N-H}\cdots\text{O}$ and $\text{O-H}\cdots\text{O}$ types (Table S2, Figure S2).

The structures of these two zinc complexes are fully consistent with the already reported structures of Zn-TDMQ5, Zn-TDMQ19 and Zn-TDMQ20, with coordination of two nitrogen atoms of the side chain in a N_2Cl_2 environment ([5a], Table 1 and Scheme 4).

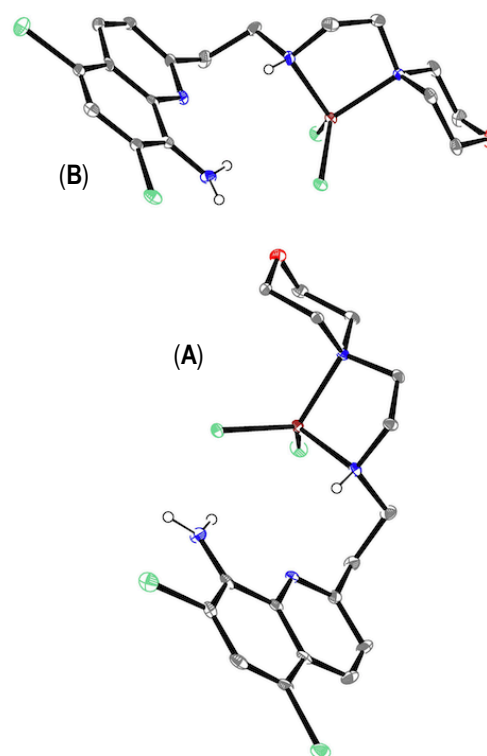
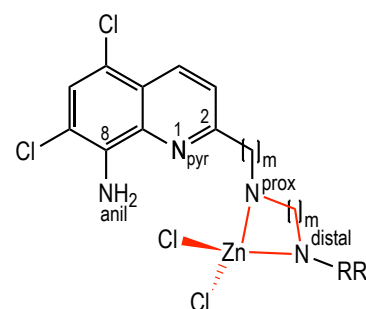


Figure 3. ORTEP drawing with ellipsoids at 30% probability of the $\text{Zn}^{\text{II}}\text{-TDMQ36}$ complex.



Scheme 4. general structures of the $\text{Zn}(\text{II})$ complexes of TDMQ5, TDMQ19, TDMQ20, TDMQ35 and TDMQ36.

X-Ray structure of Zn-TDMQ22

Single crystals of Zn-TDMQ22 were obtained by slow vapor diffusion of dichloromethane into solution of TDMQ22 and ZnCl₂ in ethanol (26 mM, TDMQ22/Zn mole ratio = 1/1) in ethanol at 4 °C. These crystals exhibited a significantly different structure than all other crystallized Zn-TDMQ complexes, with an unusual coordination number of zinc of 5. In the space group *C2/c*, in each Zn-TDMQ22 motif, Zn(II) was chelated in a distorted square plane, by the four nitrogen atoms of the ligand: N_{pyridine}, N_{aniline}, and the N_{proximal} and N_{distal} of the side chain (Figure 4). The aniline nitrogen was not deprotonated, and electroneutrality of the complex was achieved by a (–Cl–Zn^{II}Cl₃)^{2–} axial ligand bound through a bridging chloride. The length of the bonds between the chelated Zn and nitrogen atoms were quite similar, measured at 2.143, 2.095, 2.087 Å, and 2.182 for N_{pyridine}, N_{aniline}, N_{proximal} and N_{distal}, respectively. The N–Zn–N angles in the base plane were N_{pyridine}–Zn–N_{aniline} (γ) = 80.43°, N_{proximal}–Zn–N_{distal} (δ) = 84.11°, N_{aniline}–Zn–N_{distal} (β) = 98.80°, and N_{pyridine}–Zn–N_{proximal} (α) = 89.58°. The dihedral angles between N_{pyridine}–Zn–N_{aniline} and N_{proximal}–Zn–N_{distal}, N_{pyridine}–Zn–N_{aniline} and N_{pyridine}–Zn–N_{proximal}, and N_{pyridine}–Zn–N_{proximal} and N_{proximal}–Zn–N_{distal} were 28.34°, 24.08°, and 15.23°, respectively. The zinc was located at 0.380 Å above the mean plane of the four nitrogen atoms, driven outside of the N₄-plane by the bridging chloride of the axial ZnCl₄ (distance between the chelated Zn and the bridging Cl = 2.384 Å). The three-dimensional network of halogen-hydrogen bonds O–H···Cl– and N–H···Cl– giving rise to the supramolecular arrangement of Zn-TDMQ22 complex is detailed in Table S3 and Figures S3 and S4. These halogen-hydrogen bonds through the *in situ* generated (ZnCl₄)^{2–} counterion might be a driving force of the complex crystallization.

The structure of Zn-TDMQ22 differs from the X-ray structures of all other Zn-TDMQ complexes that have been obtained, in which the aminoquinoline motif does not chelate zinc which is coordinated only by the nitrogen atoms of the aliphatic side chain, in a N₂X₂ environment. It might be a special feature due to the *in situ* formation of the counterion (Cu^{II}Cl₄)^{2–} which is itself due to the high concentration of the species in the crystallization solution (26 mM).

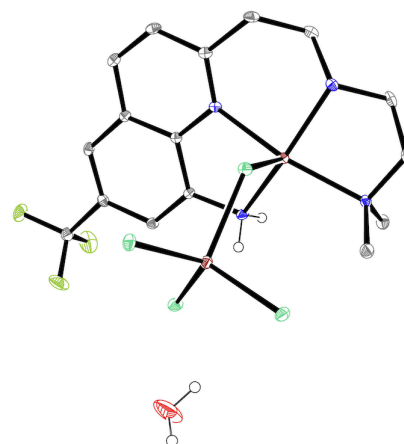


Figure 4. ORTEP drawing with ellipsoids at 30% probability of the Zn^{II}-TDMQ22 complex.

This structure, close to that of several Cu^{II}-TDMQ complexes, confirms the versatility of complexation modes of zinc, which have been reported for the 8-hydroxyquinoline derivative PBT2 [10].

Conclusion

We report here the X-ray structure of single crystals of Cu-TDMQ36, and also those of the zinc complexes of the tetradentate ligands TDMQ35, TDMQ36 and TDMQ22. Comparison with the already reported structures of other copper and zinc complexes of TDMQs [5a, 2b, 7] allow to specify the structure requirement for drugs potentially efficient to regulate copper homeostasis in the zinc-rich environment of human brain. Among the various possibilities offered by the diversity of metal chelators, we confirmed that the most suitable N4-tetradentate 8-aminoquinoline ligands to transfer copper from metal-amyloids to metal-carrier proteins, and capable of inhibiting the catalytic reduction of dioxygen produced by copper-loaded amyloids exposed to a reductant, generate strictly square planar Cu(II) complexes *in vitro*. On the other hand, the coordination of Zn(II) involving only the TDMQ side chain but not the quinoline nucleus, may explain the low affinity of these chelators for physiological concentrations of zinc.

Experimental Section

Chemicals and methods

TDMQ5, TDMQ19, TDMQ20 and TDMQ22 were prepared according to Reference 5a. TDMQ35-37 were prepared according to Reference 7. Cu(II)- and Zn(II) chloride were used as sources of metal ions.

The crystals were kept in their mother liquor until they were dipped in perfluoropolyether oil and their structure determined. The chosen crystals were mounted on a Mitegen micromount and quickly cooled down to low temperature (100 K). The selected crystals were mounted on a Bruker Kappa APEX II using a micro-focus molybdenum K α radiation ($\lambda = 0.71073 \text{ \AA}$) with a graphite monochromator and equipped with an Oxford Cryosystems Cooler Device. The unit cell determination and data integration were carried out using APEX III [11]. The structures have been solved by Direct Methods using SHELXS [12], and refined by means of least-squares procedures either on F with the aid of the program CRYSTALS [13], or on F² with the aid of

the program SHELXL2018 [12] included in the software package WinGX version 1.63 [14]. Atomic scattering factors were taken from the International Tables for X-ray crystallography [15]. Absorption correction was done using multi-scan [16]. Almost all hydrogen atoms were geometrically placed and refined using a riding model, excepted the hydrogen atoms H_2N_{aniline} , H_2O , and HN_{distal} of Zn-TDMQ22, and H_2N_{aniline} , and HN_{distal} of Zn-TDMQ35, which were located by Fourier differences and isotropically refined.

All non-hydrogen atoms were anisotropically refined. Details of the structure solution and refinements are given in the Supporting Information (CIF files) as CCDC no. 1952669 (Cu-TDMQ36), 1952670 (Zn-TDMQ36), 2112483 (Zn-TDMQ22), and 2112484 (Zn-TDMQ35). Drawing of molecules were performed with the program Mercury [17].

Preparation of single crystals for X-ray diffraction

Cu^{II}-TDMQ36. CuCl_2 in ethanol (0.97 M, 22.3 μL , 21.6 μmol) was added to TDMQ36 dissolved in a mixture of dimethylformamide and ethanol (DMF/EtOH = 0.15 mL / 0.5 mL, 10.7 mg, 21.6 μmol) containing triethylamine (TEA, 65 μmol , 3 mole equiv). The resulting solution was filtered through a polyester syringe filter (Chromafil® GF/PET-45/25). Crystals suitable for X-ray analysis were obtained by the slow evaporation of the filtered solution in air at room temperature.

Zn^{II}-TDMQ35. TDMQ35 was first neutralized extraction with dichloromethane of a solution containing TDMQ35 (hydrochloride salt, 4.95 mg, 10 μmol) and TEA (3.3 mole equiv) in water (0.6 mL). The organic layer was dried over Na_2SO_4 , filtered and concentrated to give a yellow residue of the base form of TDMQ35 base, which was dissolved in ethanol (0.45 mL). Then, ZnCl_2 in ethanol (0.97 M, 5.15 μL , 5 μmol , 0.5 mol equiv) was added and the resulting solution was filtered through a polyester syringe filter (Chromafil® GF/PET-45/25). Crystals suitable for X-ray analysis were obtained by the slow vapour diffusion of dichloromethane into the filtered solution placed at 4°C.

Zn^{II}-TDMQ36. TDMQ36 was neutralized by extraction with dichloromethane of a solution containing TDMQ36 (hydrochloride salt, 5.0 mg, 10 μmol) and TEA (3.3 mole equiv) in water (0.6 mL). The organic layer was dried over Na_2SO_4 , filtered and concentrated to give a yellow residue of the base form of TDMQ36 which was dissolved in ethanol (0.45 mL). Then, ZnCl_2 in ethanol (0.97 M, 10.3 μL , 10 μmol) was added and the resulting solution was filtered through a polyester syringe filter (Chromafil® GF/PET-45/25). Crystals suitable for X-ray analysis

were obtained by the slow vapour diffusion of dichloromethane into the filtered solution placed at 4°C.

Zn^{II}-TDMQ22. ZnCl₂ in ethanol (0.97 M, 22.5 μL, 21.8 μmol) was added to TDMQ22 (10.0 mg, 21.8 μmol) dissolved in ethanol (0.8 mL) containing TEA (3 mole equiv). The resulting solution was filtered through a polyester syringe filter (Chromafil® GF/PET-45/25). Crystals suitable for X-ray analysis were grown by the slow vapour diffusion of dichloromethane into the filtered solution placed at 4°C.

References

- [1] J. L. Cummings, M. Travis, K. Zhong, Alzheimer's disease drug-development pipeline: few candidates, frequent failures, *Alzheimer's Res. Ther.* 6 (2014) 37-43.
- [2] a) A. Robert, Y. Liu, M. Nguyen, B. Meunier, Regulation of copper and iron homeostasis by metal chelators: A possible chemotherapy for Alzheimer's disease, *Acc. Chem. Res.* 48 (2015) 1332-1339; b) Y. Liu, M. Nguyen, A. Robert, B. Meunier, Metal ions in Alzheimer's disease: A key role or not? *Acc. Chem. Res.* 52 (2019) 2026-2035.
- [3] K. J. Barnham, A. I. Bush, Biological metals and metal-targeting compounds in major neurodegenerative diseases, *Chem. Soc. Rev.* 43 (2014) 6727-6749.
- [4] R. A. Cherny, C. S. Atwood, M. E. Xilinas, D. N. Gray, W. D. Jones, C. A. McLean, K. J. Barnham, I. Volitakis, F. W. Fraser, Y.-S. Kim, X. Huang, L. E. Goldstein, R. D. Moir, J. T. Lim, K. Beyreuther, H. Zheng, R. E. Tanzi, C. L. Masters, A. I. Bush, Treatment with a copper-zinc chelator markedly and rapidly inhibits beta-amyloid accumulation in Alzheimer's disease transgenic mice, *Neuron* 30 (2001) 665-676.
- [5] a) W. Zhang, D. Huang, M. Huang, J. Huang, D. Wang, X. Liu, M. Nguyen, L. Vendier, S. Mazères, A. Robert, Y. Liu, B. Meunier, Preparation of new tetradentate copper chelators as potential anti-Alzheimer agents, *ChemMedChem* 13 (2018) 684-704; b) W. Zhang, Y. Liu, C. Hureau, A. Robert, B. Meunier, N₄-Tetradentate chelators efficiently regulate copper homeostasis and prevent ROS production induced by copper-amyloid-β₁₋₁₆, even in the presence of an excess of zinc, *Chem. Eur. J.* 24 (2018) 7825-7829; c) J. Huang, M. Nguyen, Y. Liu, A. Robert, B. Meunier, The TDMQ regulators of copper homeostasis do not disturb Cu,Zn-SOD and tyrosinase activity, nor the Cu(III) cofactor vitamin B12, *Eur. J. Inorg. Chem.* (2019) 1384-1388.

- [6] J. Zhao, Q. Shi, H. Tian, Y. Li, Y. Liu, Z. Xu, A. Robert, Q. Liu, B. Meunier, TDMQ20, a specific copper chelator, reduces memory impairments in AD-mouse models, *ACS Chem. Neurosci.* 12 (2021) 140-149.
- [7] Why is tetradentate coordination essential for potential copper homeostasis regulators in Alzheimer's disease?
Y. Li, M. Nguyen, M. Baudoin, L. Vendier, Y. Liu, A. Robert, B. Meunier, *Eur. J. Inorg. Chem.* (2019) 4712-4718.
- [8] M. Nguyen, C. Bijani, N. Martins, B. Meunier, A. Robert, Transfer of copper from an amyloid to a natural copper-carrier peptide with a specific mediating ligand, *Chem. Eur. J.* 21 (2015) 17085-17090.
- [9] T. Dudev, C. Lim, Tetrahedral vs octahedral zinc complexes with ligands of biological interest: A DFT/CDM study, *J. Am. Chem. Soc.* 122 (2000) 11146-11153.
- [10] M. Nguyen, L. Vendier, J.-L. Stigliani, B. Meunier, A. Robert, Structures of copper and zinc complexes of PBT2, a chelating agent evaluated as potential drug for neurodegenerative diseases, *Eur. J. Inorg. Chem.* (2017) 600-608.
- [11] SAINT Bruker. Bruker AXS Inc., Madison, Wisconsin, USA (2007).
- [12] G. M. Sheldrick, SHELX programmes, *Acta Crystallogr., Sect. A: Found. Crystallogr.* 64 (2008) 112-122.
- [13] P. W. Betteridge, J. R. Carruthers, K. Prout, D. J. Watkin, CRYSTALS version 12: software for guided crystal structure analysis, *J. Appl. Cryst.* 36 (2003) 1487.
- [14] L. Farrugia, WINGX - 1.63 Integrated system of Windows programs for the solution, refinement and analysis of single crystal X-ray diffraction data, *J. Appl. Crystallogr.* 32 (1999) 837-838.
- [15] International tables for X-ray crystallography, Vol IV, Kynoch press, Birmingham, England (1974).
- [16] R. Blessing, An empirical correction for absorption anisotropy, *Acta Cryst. A* 51 (1995) 33-38.
- [17] C. F. Macrae, P. R. Edgington, P. McCabe, E. Pidcock, G. P. Shields, R. Taylor, M. Towler, J. van der Streek, Mercury: visualization and analysis of crystal structures, *J. Appl. Crystallogr.*, 39 (2006) 453-457.

CrediT author statement

Youzhi Li Methodology, investigation

Michel Nguyen	Methodology, investigation
Laure Vendier	Methodology, investigation, validation, formal analysis, resources
Anne Robert	Conceptualization, validation, supervision, writing draft
Yan Liu	Conceptualization, project administration, funding acquisition
Bernard Meunier	Conceptualization, project administration, funding acquisition

Funding

This work was supported by the NSFC (grant 21502023, YL), the Guangdong Province (Program for Innovative Research Teams and Leading Talents Introduction, grant 2050205, BM), GDUT (grant 220418037, BM), and the CNRS.

Graphical abstract

